

LNF-98/030

**Local-Structure Determination in T- and T<sup>1</sup>- Phase  
Materials by 2p x-Ray-Absorption Spectra of  
La, Nd, Y, and Sr**

Z. Wu, M. Benfatto, C.R. Natoli

*Physical Review B 57, 17, 10336-10339, (1998)*

## Local-structure determination in $T$ - and $T'$ -phase materials by $2p$ x-ray-absorption spectra of La, Nd, Gd, Y, and Sr

Ziyu Wu

*Institut des Matériaux de Nantes, CNRS UMR 110, Laboratoire de Chimie des Solides, 2 rue de la Houssinière, 44072 Nantes Cedex 03, France*  
and *INFN - Laboratori Nazionali di Frascati, P.O. Box 13, 00044 Frascati, Italy*

M. Benfatto and C. R. Natoli

*INFN - Laboratori Nazionali di Frascati, P.O. Box 13, 00044 Frascati, Italy*  
(Received 13 November 1997)

In analyzing the x-ray-absorption near-edge structure (XANES) at the La, Nd, Gd, Y, and Sr  $L_3$  edges in  $T$ - and  $T'$ -phase materials, we have found a general rule that links the presence of a feature at about 20 eV from the rising edge, called  $A$  in the experimental data by Tan *et al.* [Phys. Rev. Lett. **64**, 2715 (1990)], with the geometrical arrangement around the absorbing site. The absorption spectra of  $\text{La}_{2-x}\text{Sr}_x\text{CuO}_4$ ,  $\text{Nd}_2\text{CuO}_4$ ,  $\text{Gd}_2\text{CuO}_4$ , and  $\text{YBa}_2\text{Cu}_3\text{O}_7$  compounds are analyzed by full multiple-scattering theory with complex potential of Hedin-Lundqvist type obtaining very good agreement between theory and experiments. As a result of this analysis we show that feature  $A$  in these spectra appears every time the photoabsorber has an eightfold hexahedron-type coordination with its nearest neighbors. This finding can be used to determine the rare-earth ordering in  $T^*$ -phase superconductors. [S0163-1829(98)05614-8]

$T$ - and  $T'$ - phase compounds  $\text{La}_2\text{CuO}_4$  and  $\text{Nd}_2\text{CuO}_4$ , contain square  $\text{CuO}_2$  planes. In the  $T$  phase, each copper is further coordinated by two out-of-plane oxygens, the six near-neighbor oxygens forming an elongated octahedron along the  $c$  axis.  $\text{La}_2\text{CuO}_4$  forms in an orthorhombic distortion of the  $T$  phase in which Lanthanum atoms are coordinated with *nine* oxygen atoms. In  $\text{Nd}_2\text{CuO}_4$ -type  $T'$  phase, the Cu atoms are only coordinated with four and the Neodymium ions with *eight* oxygens. They can both be doped by Sr and rare-earth elements. The resulting complexes show a rich variety of physical properties, and they are often superconductors.<sup>1-7</sup>

Although great theoretical and experimental efforts have led to important general insight into the chemical and electronic structure of the high- $T_c$  cuprates, a satisfactory understanding of the phenomenon of high-temperature superconductivity and its occurrence in the copper oxides is still far from being achieved.<sup>8</sup> The structure plays an important role in determining the superconducting properties and, consequently, a detailed understanding of it is a prerequisite to a full investigation of these properties.<sup>9</sup> Therefore, e.g., a simple rule relating the local structure around the photoabsorber to definite features in the absorption spectrum of these materials would provide a cheap and useful means for deciding about local structural arrangements, especially in cases of impurity doping.

A step forward in this direction was taken recently by Tan *et al.*<sup>1,10</sup> In an x-ray-absorption near-edge structure (XANES) study of some  $T^*$ -,  $T$ -, and  $T'$ -phase materials, both at the rare-earth  $L_3$  edge and the  $K$  of the Sr dopant, these authors suggested that a spectral feature (called peak  $A$  in their paper), appearing approximately 20 eV above the absorption edge, is related to an eightfold-coordinated absorber with two sets of four equivalent near neighbors. How-

ever, in two subsequent papers<sup>11</sup> we have contested this simple interpretation of the presence (or absence) of peak  $A$  and shown that in these compounds near-edge spectral features (and in particular peak  $A$ ) are not only related to the coordination environment of the photoabsorber but also depend on the type of final state probed by the photoelectron, the electronic configuration of the absorbing atom and the type of neighboring atoms. In particular we were able to show that multiple-scattering (MS) calculations could reproduce all the transition peaks present in the Sr  $K$ -edge XANES spectrum of the  $\text{La}_{2-x}\text{Sr}_x\text{CuO}_4$  compound, and in particular peak  $A$ , in a cluster configuration in which the dopant Sr atom is ninefold coordinated with the surrounding oxygens, contrary to the suggestion put forward by Tan *et al.*<sup>1,10</sup> In this case we found that feature  $A$  was due to a constructive interference between the outgoing photoelectron wave and waves backscattered by atoms lying in far away coordination shells, so that the crystallographic order was somehow expedient to the build up of peak  $A$ .

In an effort to gain a deeper insight into this question and in order to find cases in which the presence of this feature is clearly related to the first coordination shell around the photoabsorber, we have reexamined the rare-earth  $L_{2,3}$ -edge spectra in the  $T$ - and  $T'$ -phase compounds. Some of the experimental results by Tan *et al.*<sup>1,10</sup> are summarized in Fig. 1, where the left panel contains the  $L_3$  edges of La in  $\text{La}_2\text{CuO}_4$  [curve (a)], of Nd in  $\text{Nd}_2\text{CuO}_4$  [curve (b)] and of Gd in  $\text{Gd}_2\text{CuO}_4$  [curve (c)]; the same edges of Sr in  $\text{SrF}_2$  [curve (a)] and of Y in  $\text{YBa}_2\text{Cu}_3\text{O}_7$  [curve (b)] are shown in the right panel.<sup>12,13</sup> The arrows indicate peak  $A$ .

As in our two previous papers,<sup>11</sup> our calculations are based on one-electron multiple-scattering theory.<sup>14</sup> The Coulomb part of the potential is built according to the Mattheiss prescription<sup>15</sup> by superimposing neutral atomic charge

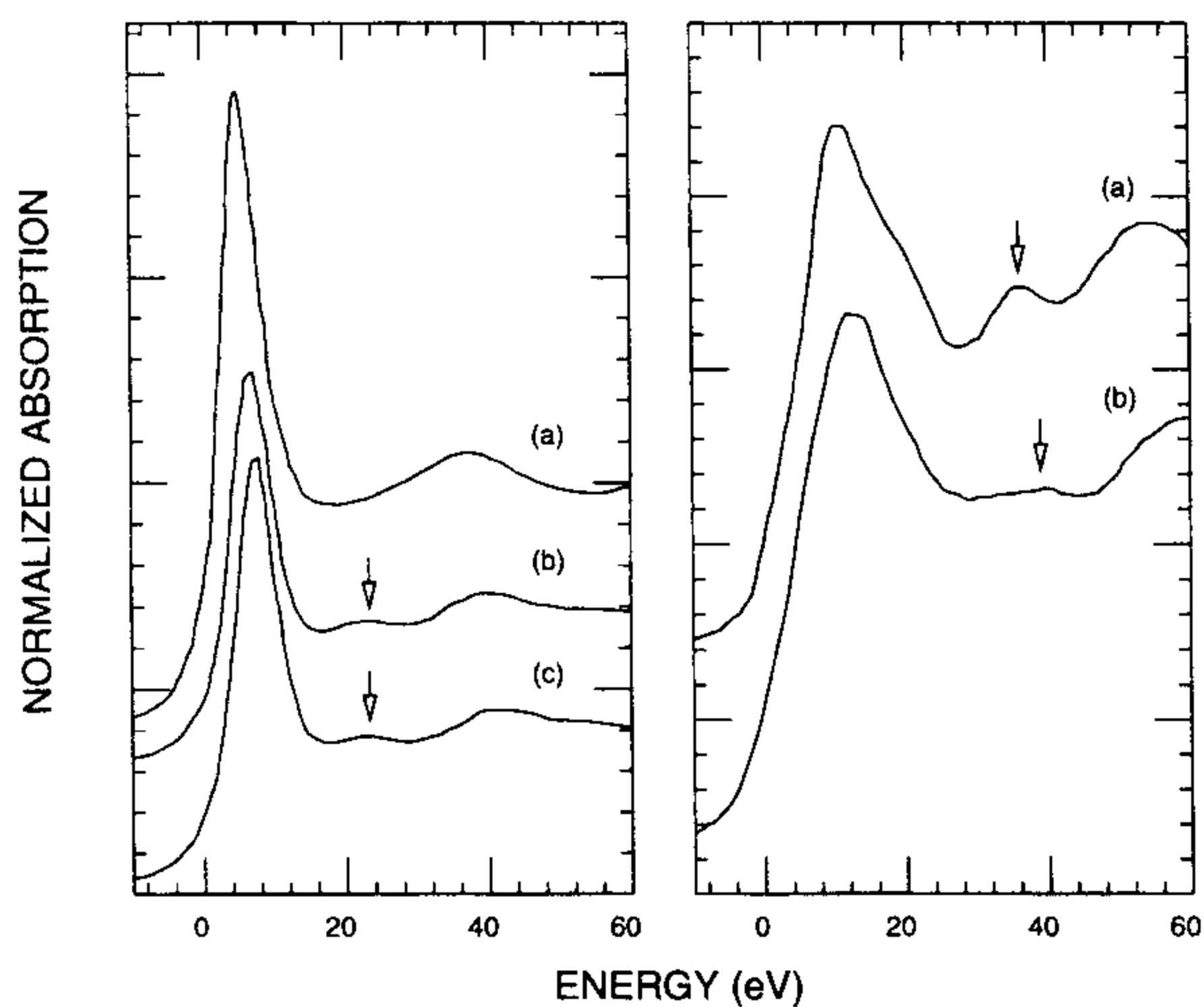


FIG. 1. The experimental  $L_3$ -edge XANES spectra measured by Tan *et al.* (Ref. 1). Left panel: (a) La  $L_3$  of  $\text{La}_2\text{CuO}_4$  ( $T$  phase); (b) Nd  $L_3$  of  $\text{Nd}_2\text{CuO}_4$  ( $T'$  phase); (c) Gd  $L_3$  of  $\text{Gd}_2\text{CuO}_4$  ( $T'$  phase). Right panel: (a) Sr  $L_3$  in  $\text{SrF}_2$ ; (b) Y  $L_3$  in  $\text{YBa}_2\text{Cu}_3\text{O}_7$ .

densities obtained from the Clementi-Roetti table and the Hermann-Skillman wave functions for heavy atoms ( $Z > 54$ ). This method, in general, is known to provide charge distributions reasonably close to those obtained by self-consistent calculation for metallic and covalent systems (see last quotation of Ref. 14). For the exchange-correlation part of the potential we use the complex Hedin-Lundqvist (HL) self-energy<sup>16</sup> whose imaginary part gives the amplitude attenuation of the excited photoelectron due to the extrinsic inelastic losses.<sup>17</sup> The calculated spectra are further convoluted with a Lorentzian shaped function with a full width  $\Gamma_h \approx 1.5$  eV for Sr and Y atoms, 3.5 eV for La, Nd, and Gd, respectively, to account for the core hole lifetime.<sup>18</sup> We have chosen the muffin-tin radii according to the Norman criterion<sup>19</sup> and have allowed a 10% overlap between contiguous spheres to simulate the atomic bond. The  $z$  axis in all our calculations is along the  $c$  axis of the compounds.

In Fig. 2 we present our theoretically calculated spectra at

TABLE I. The nearest-neighbor atoms.

Atom	$\text{YBa}_2\text{Cu}_3\text{O}_7$			$\text{SrF}_2$			
	$x$	$y$	$z$	Atom	$x$	$y$	$z$
Y	0.0	0.0	0.0	Sr	0.0	0.0	0.0
O1	0.0	-1.932	1.431	F1	1.447	1.447	1.447
O1	-1.931	0.0	1.431	F1	-1.447	1.447	1.447
O1	1.931	0.0	1.431	F1	1.447	-1.447	1.447
O1	0.0	1.932	1.431	F1	-1.447	-1.447	1.447
O2	0.0	-1.932	-1.431	F2	1.447	1.447	-1.447
O2	-1.931	0.0	-1.431	F2	-1.447	1.447	-1.447
O2	1.931	0.0	-1.431	F2	1.447	-1.447	-1.447
O2	0.0	1.932	-1.431	F2	-1.447	-1.447	-1.447

$\text{Nd}_2\text{CuO}_4$			$\text{La}_{2-x}\text{Sr}_x\text{CuO}_4$				
Nd	0.0	0.0	0.0	La(Sr)	0.0	0.0	0.0
				O	0.0	0.0	2.356
O1	1.975	0.0	1.219	O1	1.890	0.0	-1.845
O1	-1.975	0.0	1.219	O1	-1.890	0.0	-1.845
O1	0.0	1.975	1.219	O1	0.0	1.890	-1.845
O1	0.0	-1.975	1.219	O1	0.0	-1.890	-1.845
O2	1.975	0.0	-1.798	O2	1.890	1.890	0.568
O2	-1.975	0.0	-1.798	O2	-1.890	1.890	0.568
O2	0.0	1.975	-1.798	O2	1.890	-1.890	0.568
O2	0.0	-1.975	-1.798	O2	-1.890	-1.890	0.568

Y, Sr, Nd, and Gd  $L_3$  edges for four different compounds and compare them with the experimental data. All the absorbers (at the center of the respective clusters with a radius of about 5 Å) are eightfold coordinated with oxygen or fluorine nearest neighbors forming an octahedronlike structure,<sup>20-22</sup> i.e., two sets of four equivalent ligands (with the same  $x$  and  $y$  coordinates) placed on two different  $z$  planes, as illustrated in Table I. Panel (a) compares the calculated Yttrium  $L_3$  XANES spectrum in  $\text{YBa}_2\text{Cu}_3\text{O}_7$  compound with its experimental counterpart. Similarly panel (b) shows Sr  $L_3$  XANES spectra of  $\text{SrF}_2$ . Nd and Gd  $L_3$  edges

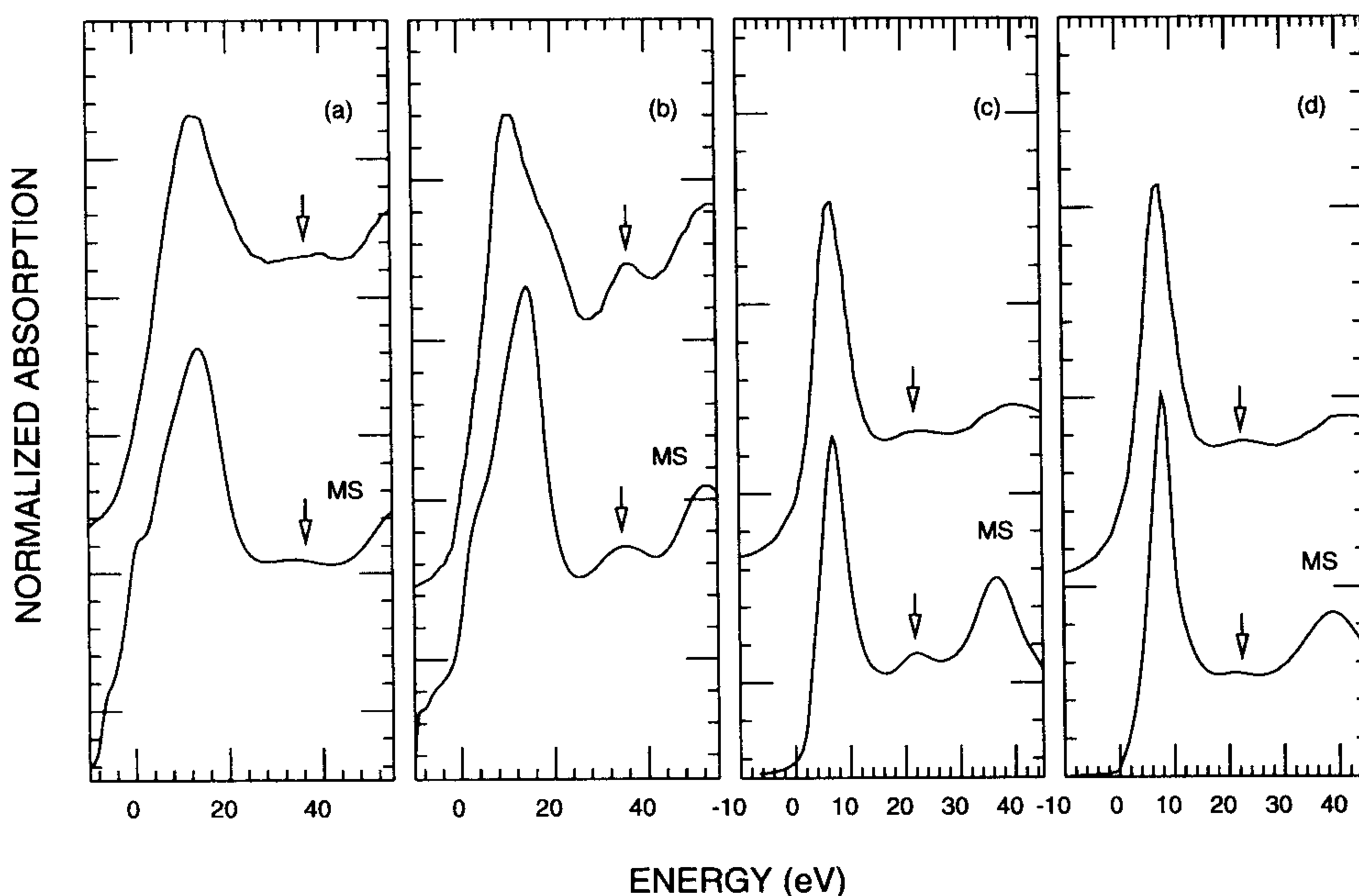


FIG. 2. Comparison between the experimental and calculated XANES spectra of (a) Y  $L_3$  edge in  $\text{YBa}_2\text{Cu}_3\text{O}_7$ ; (b) Sr  $L_3$  edge in  $\text{SrF}_2$ ; (c) Nd  $L_3$  edge in  $\text{Nd}_2\text{CuO}_4$ ; and (d) Gd  $L_3$  edge in  $\text{Gd}_2\text{CuO}_4$ .

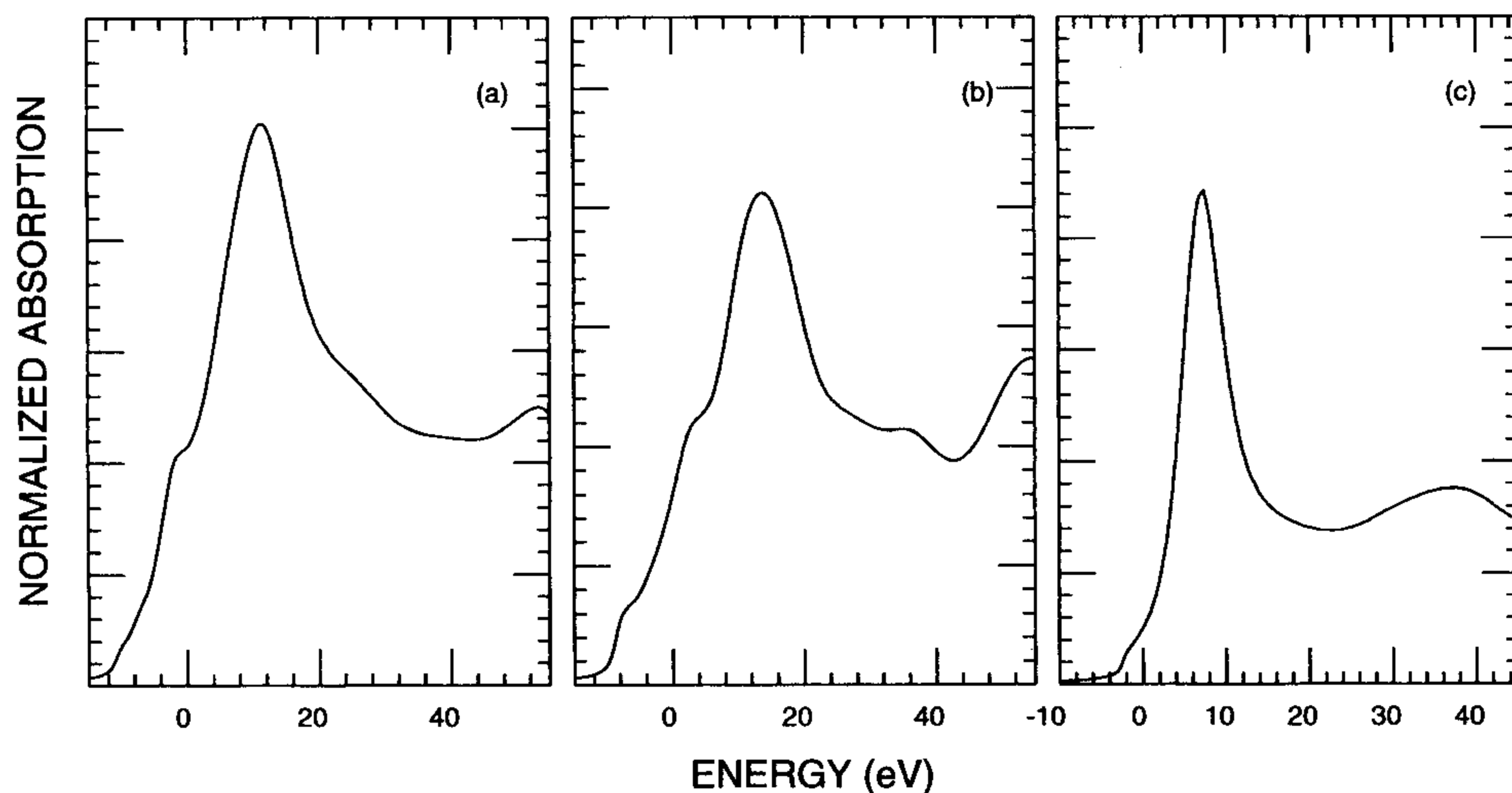


FIG. 3. Theoretical XANES spectra of (a) Y  $L_3$  edge, (b) Sr  $L_3$  edge, and (c) Nd  $L_3$  edge, in the same compounds as in Fig. 2, obtained using the same atomic cluster except for a  $45^\circ$  rotation of the upper plane formed by ligand atoms, e.g., O1 (F1) in Table I, with respect to the lower one defined by the O2 (F2) atoms.

for  $\text{Nd}_2\text{CuO}_4$  and  $\text{Gd}_2\text{CuO}_4$  compounds are shown in panels (c) and (d), respectively. All calculated spectral features are in reasonably good agreement with those of the experimental spectra both in relative amplitude and energy position. Feature A, again indicated by an arrow, is very well defined in all calculated spectra.

In order to gain a better insight into the origin of feature A we present in Fig. 3 three calculations for Y [panel (a)], Sr [panel (b)], and Nd [panel (c)]  $L_3$  edges in the same compounds, obtained using the same atomic cluster as in Fig. 2 except for a  $45^\circ$  rotation of the upper plane formed by one set of the four equivalent oxygen (fluorine) atoms, e.g., O1 (F1) in Table I, with respect to the lower one defined by the O2 (F2) atoms. The nearest-neighbor configuration of the absorber in all clusters is now similar to that of La in  $\text{La}_2\text{CuO}_4$  (Refs. 23–25) but with an eightfold coordination, without one apical oxygen. Feature A does not survive. This finding clearly indicates that feature A is the result of constructive interference between the two oxygen (fluorine) planes, being sensitive to the relative positions of these atoms.

As a counter example we present in Fig. 4 the calculations of Sr and La  $L_3$  edges XANES spectra in  $T$ -phase compound  $\text{La}_{2-x}\text{Sr}_x\text{CuO}_4$ .<sup>23,24</sup> In Fig. 4(a) we present the results of Sr  $L_3$ -edge XANES spectrum which does not show feature A

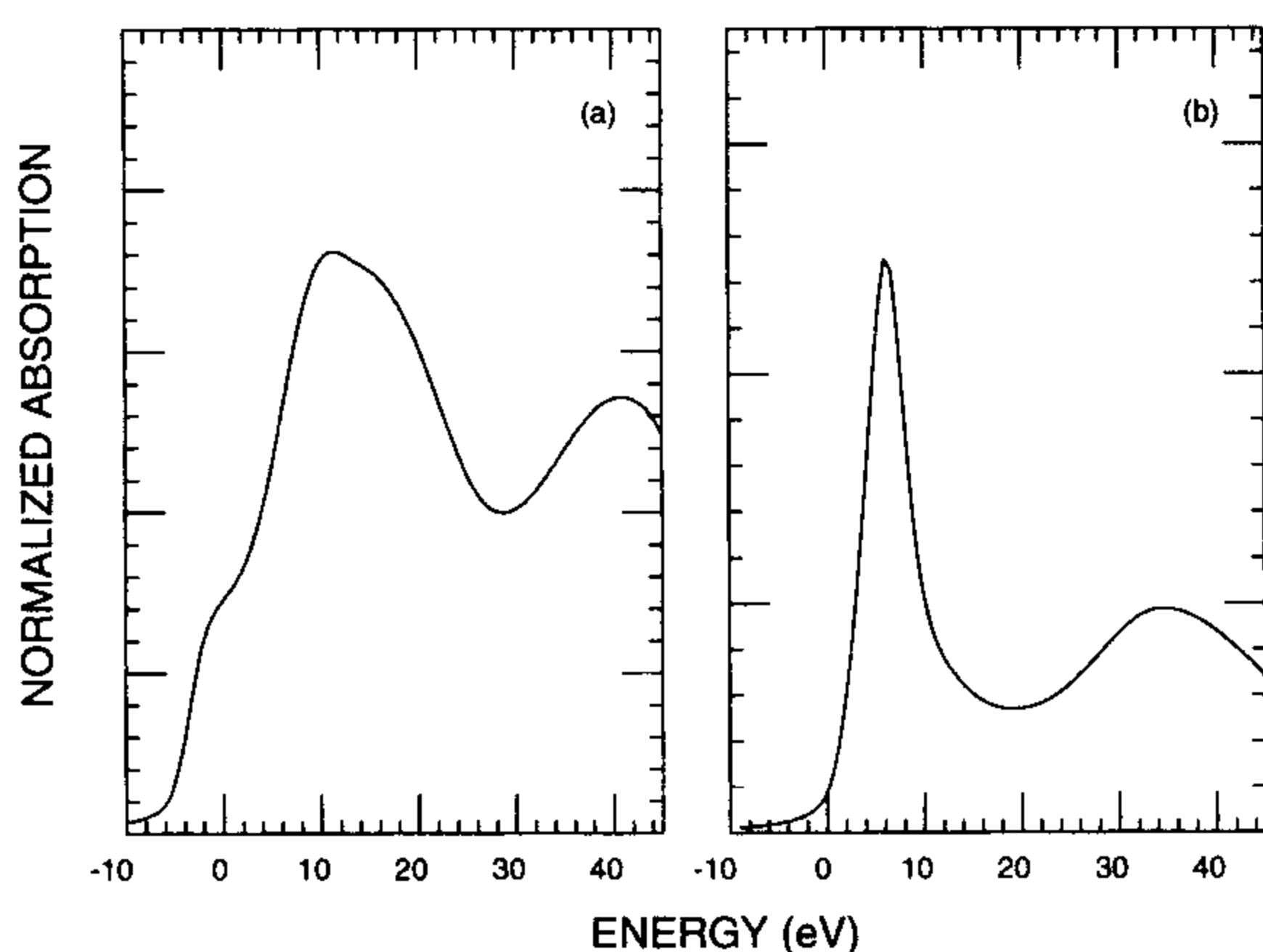


FIG. 4. Theoretical XANES spectra at Sr  $L_3$  edge [panel (a)] and La  $L_3$  edge [panel (b)] of  $\text{La}_{2-x}\text{Sr}_x\text{CuO}_4$  compounds. Peak A is absent in both calculations.

and incidentally is completely different from  $K$ -edge spectrum,<sup>1,11</sup> where peak A is present. The absence of peak A at the  $L_3$  edge is an indication that the type of projected density of state has a bearing on the appearance of this feature. Figure 4(b) gives La  $L_3$  edge spectra with the same structure. Good agreement with the experimental data, shown in Fig. 1, is obtained in calculations. Again peak A is absent, showing the relation between its presence and the hexahedronlike coordination of the photoabsorber with its nearest neighbors.

In order to demonstrate that feature A is not sensitive to the coordination number of the nearest-neighbor shell, whether 8 or 9, but only to the relative orientation of the upper and lower planes we present in Fig. 5 two test calculations of La  $L_3$  edge in  $\text{La}_2\text{CuO}_4$  and Nd  $L_3$  edge in  $\text{Nd}_2\text{CuO}_4$ . In the first case [curve (a)], we have rotated arti-

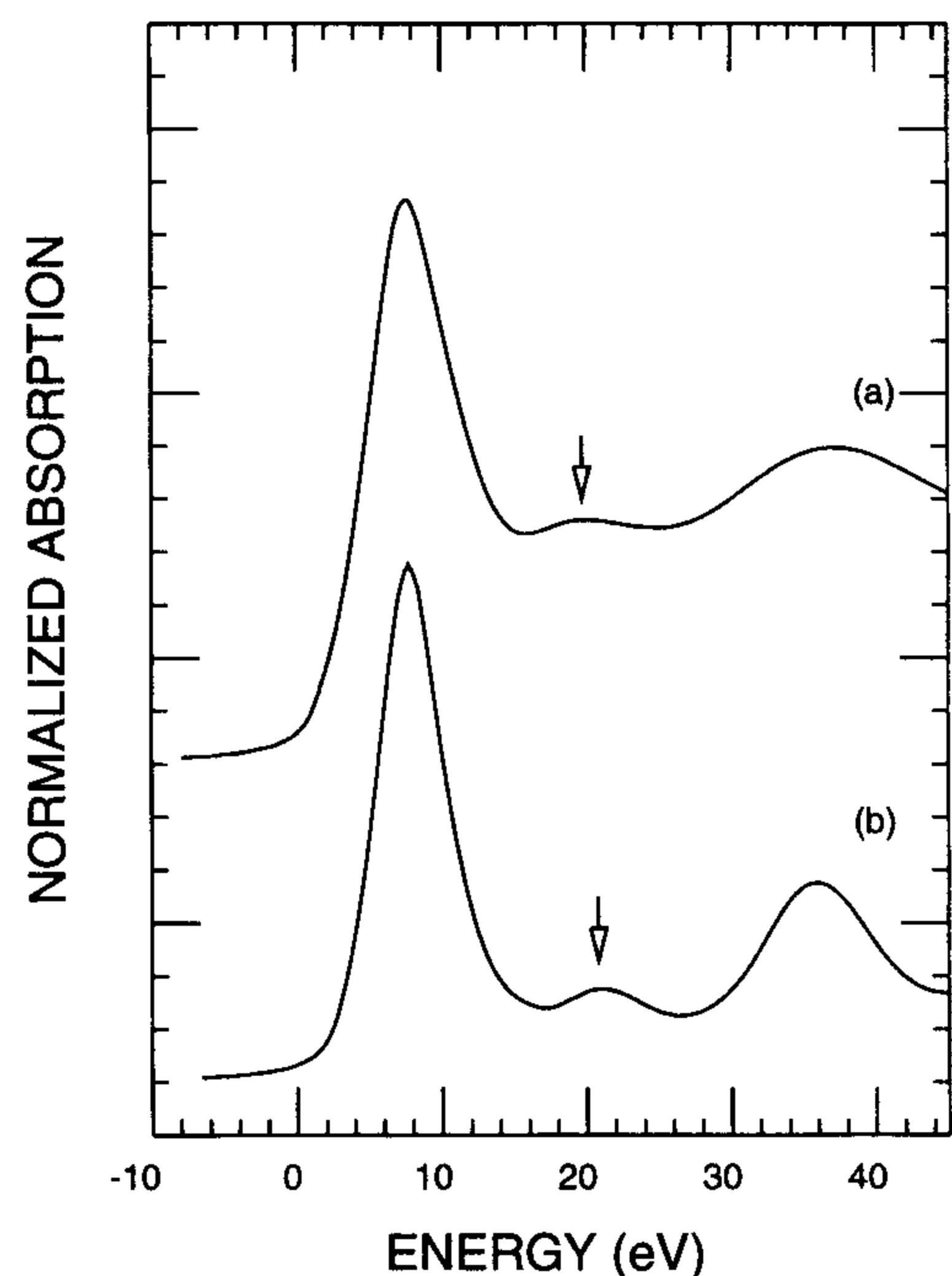


FIG. 5. (a) Theoretical La  $L_3$  XANES spectrum of  $\text{La}_2\text{CuO}_4$  using a cluster in which one nearest O1 plane is rotated by  $45^\circ$  respect to O2 plane; (b) Nd  $L_3$  XANES for  $\text{Nd}_2\text{CuO}_4$  by using a cluster with one extra apical oxygen.

ficially the O1 upper plane (see Table I for reference) by  $45^\circ$  with respect to O2 lower plane while keeping the remaining atoms in the cluster in their normal crystallographic positions. In this way the coordination number around the absorber is still nine while the atoms located in the upper and lower planes have the same  $x, y$  coordinates. As shown in curve (a), feature A reappears in the spectrum at about 20 eV from the rising edge as in the curves (b) and (c) of Fig. 1. In the second case [curve (b)] we add artificially an apical oxygen atom at about 2.3 Å away from Nd along  $z$  axis. Peak A is not suppressed although now the photoabsorber is ninefold coordinated.

Finally, to assess the effect of local deviations from average crystallographic positions on feature A, we have also made several calculations (that, for brevity, we do not report in the paper) obtained by moving in different way the eight oxygen atoms in the hexahedral coordination. We have ob-

served that feature A is almost unchanged for any reasonable deviation, within about 0.15 Å, from crystallographic positions.

In conclusion, we have presented theoretical calculations of x-ray-absorption near-edge structure at the Sr, Y, La, Nd, and Gd  $L_3$  edges in  $T$ - and  $T'$ -compounds obtaining results in good agreement with experimental spectra, when available, both in relative amplitude and energy position. In these spectra feature A appears only in the case where the first atomic shell surrounding the photoabsorber has an hexahedronlike symmetry due to a constructive interference of MS signals between ligands located on the two lower and upper planes along the  $z$  axis. This behavior seems to be a general rule in these compounds and can be used to determine the La, rare-earth elements and substitutional dopant ordering in  $T^*$ -phase superconductors.<sup>2,4,6,7,10,26</sup>

<sup>1</sup>Z.Q. Tan *et al.*, Phys. Rev. Lett. **64**, 2715 (1990).

<sup>2</sup>Y. Tokura, H. Takagi, and S. Uchida, Nature (London) **337**, 345 (1989).

<sup>3</sup>H. Muller-Buschbaum and W. Wollschlager, Z. Anorg. Allg. Chem. **414**, 76 (1975).

<sup>4</sup>S-W. Cheong, Z. Fisk, J.D. Thompson, and R.B. Schwarz Physica C **159**, 407 (1989).

<sup>5</sup>G.H. Kwei, R.B. Von Dreele, S-W. Cheong, Z. Fisk, and J.D. Thompson, Phys. Rev. B **41**, 1889 (1990).

<sup>6</sup>H. Sawa *et al.*, Nature (London) **337**, 347 (1989).

<sup>7</sup>F. Izumi *et al.*, Physica C **158**, 440 (1989).

<sup>8</sup>See, for example, *Physical Properties of High-Temperature Superconductors*, edited by D.M. Ginsberg (World Scientific, Singapore, 1988–1992), Vols. I–III.

<sup>9</sup>*Proceedings of the Conference on Lattice Effects in High- $T_c$  Superconductors*, edited by Y. BarYam *et al.* (World Scientific, Singapore, 1992).

<sup>10</sup>Z.Q. Tan *et al.*, Phys. Rev. B **42**, 4808 (1990); Z.Q. Tan *et al.*, *ibid.* **44**, 7008 (1991).

<sup>11</sup>Z.Y. Wu, M. Benfatto, and C.R. Natoli, Phys. Rev. B **45**, 531 (1992); Z.Y. Wu, M. Benfatto, and C.R. Natoli, Solid State Commun. **87**, 475 (1993).

<sup>12</sup>E.E. Alp *et al.*, Phys. Rev. B **35**, 7199 (1987); Y. Jeon *et al.*, *ibid.* **36**, 3891 (1987); A. Bianconi *et al.*, Z. Phys. B **67**, 307 (1987); F.W. Lytle *et al.*, Phys. Rev. B **37**, 1550 (1988); K.B. Garg *et al.*, *ibid.* **38**, 244 (1988); N. Kosugi *et al.*, Chem. Phys. **135**,

149 (1989); J. Guo *et al.*, Phys. Rev. B **39**, 6125 (1989); J. Guo *et al.*, *ibid.* **41**, 82 (1990).

<sup>13</sup>J. Akimitsu, S. Suzuki, M. Watanabe, and H. Sawa, Jpn. J. Appl. Phys. **27**, L1859 (1988).

<sup>14</sup>P.A. Lee and J.B. Pendry, Phys. Rev. B **11**, 2795 (1975); C.R. Natoli *et al.*, Phys. Rev. A **22**, 1104 (1980); P.J. Durham *et al.*, Comput. Phys. Commun. **25**, 193 (1982); C.R. Natoli and M. Benfatto, J. Phys. (Paris), Colloq. **47**, C8-11 (1986); P.J. Durham, in *X-ray Absorption: Principles, Applications, Techniques of EXAFS, SEXAFS, XANES*, edited by R. Prinz and D. Koningsberger (Wiley, New York, 1988).

<sup>15</sup>L. Mattheiss, Phys. Rev. **134**, A970 (1964).

<sup>16</sup>S.H. Chou, J.J. Rehr, E.A. Stern, and E.R. Davidson, Phys. Rev. B **35**, 2604 (1987), and references therein.

<sup>17</sup>T.A. Tyson, K.O. Hodgson, C.R. Natoli, and M. Benfatto, Phys. Rev. B **46**, 5997 (1992).

<sup>18</sup>J.C. Fuggle and J.E. Inglesfield, *Unoccupied Electronic States, Topics in Applied Physics* (Berlin, Springer, 1992), Appendix B.

<sup>19</sup>J.G. Norman, Mol. Phys. **81**, 1191 (1974).

<sup>20</sup>K. Yavon and M. Francois, Z. Phys. B **76**, 413 (1989).

<sup>21</sup>W.F. de Jong, *General Crystallography* (Freeman, San Francisco, 1959), p. 155.

<sup>22</sup>V.B. Grande *et al.*, Z. Anorg. Allg. Chem. **428**, 120 (1977).

<sup>23</sup>C. Chaillout *et al.*, Physica C **158**, 183 (1989).

<sup>24</sup>J.D. Jorgensen *et al.*, Phys. Rev. B **40**, 2187 (1989).

<sup>25</sup>R.J. Cava *et al.*, Phys. Rev. B **35**, 6716 (1987).

<sup>26</sup>M.F. Hundley *et al.*, Phys. Rev. B **40**, 5251 (1989).